Wiley Online Library
Early View publication on www.wileyonlinelibrary.com
(issue and page numbers not yet assigned;
citable using Digital Object Identifier – **DOI**)

Phys. Status Solidi B, 1–5 (2016) / **DOI** 10.1002/pssb.201600546

Part of Special Issue on
Single-Electron Control in Solid-State Devices

physica status solidi b
www.pss-b.com
basic solid state physics

Heat dissipation and fluctuations in a driven quantum dot

Andrea Hofmann[*,1], Ville F. Maisi[1], Julien Basset[1], Christian Reichl[1], Werner Wegscheider[1], Thomas Ihn[1], Klaus Ensslin[1], and Christopher Jarzynski[*,2]

[1] Laboratory for Solid State Physics, ETH Zurich, Switzerland
[2] Department of Chemistry and Biochemistry and Institute for Physical Science and Technology, University of Maryland, USA

Received 15 August 2016, revised 8 October 2016, accepted 18 October 2016
Published online 8 December 2016

Keywords fluctuation theorems, GaAs/AlGaAs, heat, quantum dots, single-electron tunneling, work

[*] Corresponding author: e-mail andrea.hofmann@phys.ethz.ch, Phone: +41 44 63 32 312, Fax: +41 44 63 31 146

While thermodynamics is a useful tool to describe the driving of large systems close to equilibrium, fluctuations dominate the distribution of heat and work in small systems and far from equilibrium. We study the heat generated by driving a small system and change the drive parameters to analyze the transition from a drive leaving the system close to equilibrium to driving it far from equilibrium. Our system is a quantum dot in a GaAs/AlGaAs heterostructure hosting a two-dimensional electron gas. The dot is tunnel-coupled to one part of the two-dimensional electron gas acting as a heat and particle reservoir. We use standard rate equations to model the driven dot–reservoir system and find excellent agreement with the experiment. Additionally, we quantify the fluctuations by experimentally testing the theoretical concept of the arrow of time, predicting our ability to distinguish whether a process goes in the forward or backward drive direction.

1 Introduction While equilibrium thermodynamics is powerful in describing the energy balance in large systems [1], fluctuations need to be taken into account when driving small systems away from equilibrium. Over the past two decades, the understanding of non-equilibrium thermodynamics has been enhanced by fluctuation theorems such as the Jarzynski and Crooks relations [2–4], and their quantum extensions [5–8]. These results reveal that fluctuations in a system driven arbitrarily far from equilibrium can be related to a very basic equilibrium quantity, the free energy of the system. Effectively, they allow us to write statements of the second law of thermodynamics, for small systems, as equalities rather than inequalities. Experimental tests have verified these predictions in the classical [9–18] as well as the quantum regime [19, 20]. Although on average, the second law of thermodynamics is valid, it might be violated in single realizations of a process in the presence of fluctuations.

We study in detail the transition from equilibrium to non-equilibrium in the example of dissipation caused by single electrons in a semiconductor quantum dot coupled to a reservoir. A suitable gate voltage can dynamically drive the single-particle states of the quantum dot with respect to the Fermi levels of the reservoirs. The dissipation is measured for every single drive realization, which makes a statistical analysis of the distribution possible and enables us to characterize the fluctuations. Depending on whether the drive is slow or fast compared to the tunneling rates between dot and reservoir, the process can be considered to be equilibrium or non-equilibrium. We show how the resulting distribution of dissipation resembles a Gaussian shape near equilibrium, and we explain the less regular curve and the origin of the sharp features away from equilibrium. Finally, we use our experiments to verify a theoretical prediction that, in effect, quantifies the ability to determine the direction of the arrow of time, in small systems driven away from equilibrium [21].

2 Experimental In our experiment, we grow a GaAs/AlGaAs heterostructure to host a two-dimensional electron system 90 nm below the surface. We define a quantum dot by applying negative voltages to top-gates, as shown in Fig. 1a, thereby depleting the two-dimensional electron gas below. The confinement gives rise to a spectrum with typical single-particle level spacings of the order of 100 μeV. The Coulomb repulsion between electrons in the quantum dot introduces an additional energy splitting of the order of 1 meV which prevents a second electron from entering the quantum dot at the same energy, and allows for studying tunneling processes of single electrons between the dot and the reservoir.

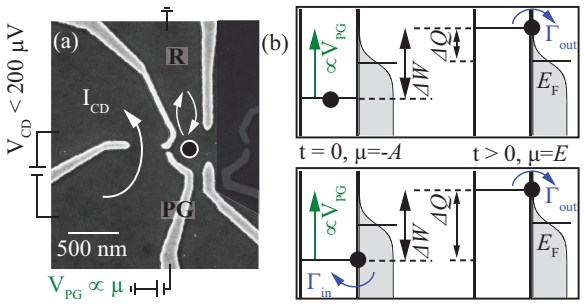

Figure 1 Experimental setup. (a) shows a scanning electron micrograph of a sample with the same lithographic design as was used for our experiment. An electron, drawn in black, can tunnel back and forth between the quantum dot and the reservoir "R". The current I_{CD} measures the occupation of the dot. The schematics of the dot–reservoir system in (b) show how work and heat are defined in our experiment. The upper panel shows a realization where the quantum dot is occupied in the beginning, hence $\Delta Q \leq A$. In the lower panel, the dot is empty at $t = 0$, and a tunneling event at small $t > 0$ time can lead to $|\Delta Q| \approx 2A$.

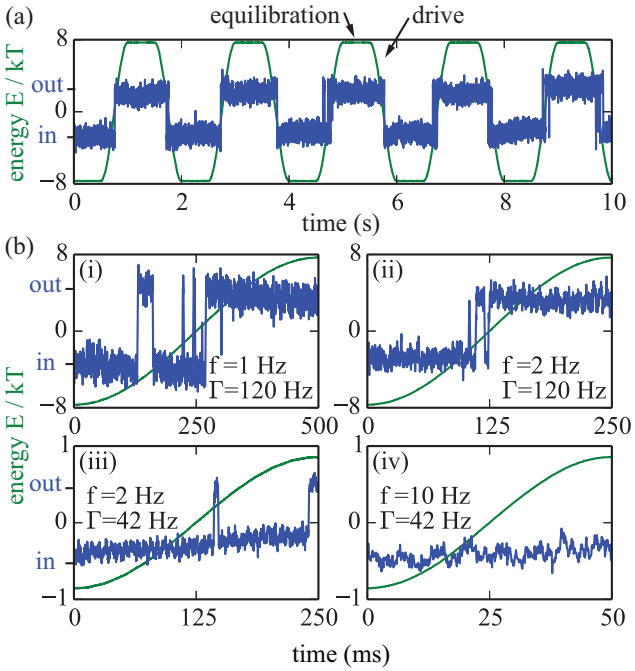

Figure 2 Drive realizations. In (a), a full time trace of ten seconds shows the energy of the quantum dot (green) being driven between $\pm 8\,kT$, as well as the equilibration periods in between. The charge detector current (blue) meanwhile monitors the occupation of the dot. In (b), we plot realizations of the drive for different frequencies, amplitudes, and tunneling rates.

For this, we utilize the current I_{CD} through a nearby channel, which is sensitive to changes in the occupation of the quantum dot [22, 23]. The quantum dot is tunnel-coupled to one region of the two-dimensional electron system (labeled "R" in Fig. 1a) acting as a heat and particle reservoir. The reservoir is described by a Fermi distribution with a Fermi energy E_F and a temperature $T = 40$ mK corresponding to an energy of 3.4 µeV. The temperature has been extracted from the width of a Coulomb resonance, which measures the thermal broadening of the Fermi distribution in the reservoir [24, 25].

The schematic illustrations in Fig. 1b show the lowest-lying electrochemical potential μ of the quantum dot, together with the reservoir Fermi distribution. In thermodynamic equilibrium, if $\mu \ll E_F$, the state at μ is occupied, while it is empty for $\mu \gg E_F$. If the energy of the dot level is within an energy window of about $4kT$ around the reservoir Fermi energy, the electron is allowed to statistically tunnel back and forth between the dot and the reservoir, at a tunneling rate which we tune to about 50 Hz. Due to the two-fold spin-degeneracy of the lowest energy level [26, 27], the tunneling-in rate, Γ, is twice as large as the tunneling-out rate, $\Gamma_{out} = 2\Gamma$ [28, 29]. By measuring the tunneling rates in thermodynamic equilibrium we probe the Fermi function of the electron reservoir, which provides the energy scale kT in units of applied gate voltage, as described in Ref. [18].

3 Heat and work in a driven quantum dot An arbitrary-wave form generator connected to the gate "PG" shifts the energy of μ with a time-periodic wave-form shown in green in Fig. 2a. We distinguish two sections in this wave-form, namely a waiting time of 0.5 s (flat sections) which allows the quantum dot to reach thermal equilibrium with the reservoir, and the drive (sections with finite slope). The drive consists of half a period of a sine with a frequency f and an amplitude A. Over the course of the entire measurement, we monitor the occupation (empty = "out", occupied = "in") of the dot with the charge detector current, as shown in blue in Fig. 2.

In the following, we analyze the dissipation and work attributed to driving the quantum dot level from $\mu = -A$ to $\mu = A$. Many hundreds of time traces are recorded for a given parameter setting f, A, Γ. An example of such a time trace is shown in Fig. 2a. Small energy drifts of the quantum dot due to its environment are taken care of by readjusting gate voltages regularly such that the average dot occupation stays constant. Different realizations of the dot occupation $q(E)$ for different parameter settings are plotted in Fig. 2b.

If the level is occupied, work ΔW is performed on the electron in the dot [30, 10] while the level is shifted in energy, as shown in Fig. 1b. Through an elastic tunneling process, the electron can leave the dot and relax in the reservoir. The dissipation ΔQ in the relaxation process equals the energy difference $E(t) - E_F$ between the dot level at the time t of the tunneling event and the reservoir Fermi energy [30, 10]. With the measured parameter $q(E)$ describing the occupation (empty = "out" = 0, occupied = "in" = 1) of the quantum dot at a certain energy E, as obtained from I_{CD} traces, these considerations allow us to determine the total work performed on the quantum dot and the total dissipation in the reservoir within one section of the drive by calculating

$$\Delta W = \int_{E=-A}^{E=A} q(E)\mathrm{d}E, \tag{1}$$

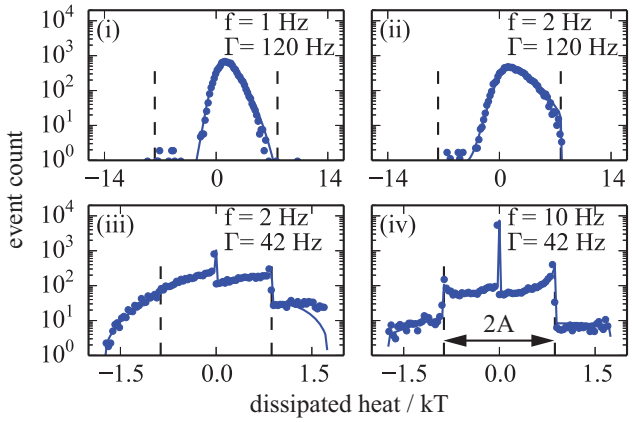

Figure 3 Distributions of dissipated heat for the upward (forward) drive direction and drive settings as described in Fig. 2b. The circles are experimental values, and the solid lines are master-equation simulations without free parameters.

$$\Delta Q = \int_{E=-A}^{E=A} \left(-\frac{\mathrm{d}q}{\mathrm{d}E}\right) E \mathrm{d}E. \tag{2}$$

The derivative $-\mathrm{d}q/\mathrm{d}E$ is non-zero only at energies, where a tunneling event occurs, and is positive for tunneling-out and negative for tunneling-in events.

In most cases, the dot is occupied when the drive starts at $\mu = -A$. When μ is driven up in energy and comes closer to the reservoir Fermi energy, electron tunneling events between the dot and the reservoir are observed, as is visible in the charge detector signal (blue) in Fig. 2. The number of events is larger for large tunneling rate Γ and slow drive frequency f.

4 Heat distribution The ensemble of several thousand realizations for each parameter setting allow for a statistical analysis of the dissipation [17, 31, 18]. The individual realizations shown in Fig. 2b are typical traces corresponding to the distributions shown in the four panels of Fig. 3.

In Fig. 3, the distribution shown in panel (i) has an almost Gaussian shape, as expected for a nearly static drive with large amplitude but low frequency. After the equilibration period, at $\mu = -A$, the quantum dot is occupied with high probability. The low frequency drive and high tunneling rate keeps the dot–reservoir system close to equilibrium during the full drive time, leading to the Gaussian shape [17, 31, 16]. Due to the large number of tunneling events, the dissipation scatters around a mean value of zero, with the variance depending on the temperature [32]. With the dot occupied in the beginning of the drive, the maximum possible dissipation is $\Delta Q = A$.

We compare the experimental distribution with a simple rate equation model [10]. The model is fully defined by the drive parameters f, A, the tunneling rate Γ, and the conversion factor between voltage on "PG" to energy. All these parameters are known from the experiment, as described also in Ref. [18]. The initial condition of the drive is set by the probability $p_{\mathrm{in}}(E = -A)$ of the quantum dot level μ to be occupied at the energy $E = -A$, which can be directly calculated from the partition function $Z(E = -A)$ of the quantum dot. The relevant single-particle energies are $\epsilon_0 = 0$ for the empty dot and $\epsilon_{1,2} = -A$ for each of the two spin-degenerate states where an electron occupies the dot. This gives

$$Z(E = -A) = \sum_i e^{-\frac{\epsilon_i}{kT}} = 1 + 2e^{\frac{A}{kT}}, \tag{3}$$

$$p_{\mathrm{in}}(E = -A) = \frac{2}{Z} e^{\frac{A}{kT}}, \tag{4}$$

$$p_{\mathrm{out}}(E = -A) = 1/Z. \tag{5}$$

We plot the result from the rate equation simulation as solid lines in Fig. 3 and find excellent agreement to the measured data.

For the second distribution, shown in panel (ii), the drive amplitude A and tunneling rate Γ are equal to those in (i), but the drive frequency f is doubled. This leads to an increased frequency of measuring positive dissipation: according to Eq. (2), positive contributions to the dissipation result from electrons tunneling into the quantum dot at negative energies ($\mu < E_{\mathrm{F}}$), and electrons tunneling out of the quantum dot at positive energies ($\mu > E_{\mathrm{F}}$). Considering that tunneling-in (-out) only occurs if an occupied (free) state is available in the reservoir, it becomes clear that positive dissipation is more probable.

For the distribution shown in panel (iii), the tunneling rate has been decreased by a factor of three, while the drive frequency has been kept equal. Effectively, this decreases the number of tunneling events and drives the dot further out of equilibrium with respect to the reservoir. As a result, sharp features appear at $\Delta Q = 0, A$. While the peak at zero dissipation will be discussed below, let us concentrate first on the sharp step. A realization with $\Delta Q \approx A$ is shown in Fig. 2b (iii). The dot is occupied in the beginning and the electron tunnels out at high energy $E \approx A$, leading to dissipation of about A. The tunneling events in-between are close to each other and therefore do not contribute significantly to the total dissipation. These realizations are likely because of the fast drive, but also the shape of the drive: the sinusoidal form enhances the probability for the electron to tunnel out at high energy. On the other hand, dissipation $\Delta Q > A$ occurs only in realizations where the dot is empty in the beginning of the drive, which is suppressed by $p_{\mathrm{in}}/p_{\mathrm{out}} = 2\exp(A/kT)$. Due to the lower drive amplitude in panel (iii) compared to (i) and (ii), a significant number of events are observed with large dissipation.

Interestingly, the twofold degeneracy of the dot energy level also influences the shape of the distribution. The probabilities for an empty and occupied dot are equal at $E = kT\ln(2)$. Therefore, if the drive is symmetric around the Fermi energy, the heat distribution has a different shape for the drive upwards in energy than downwards in energy, although all other drive parameters are equal, as illustrated in Ref. [18].

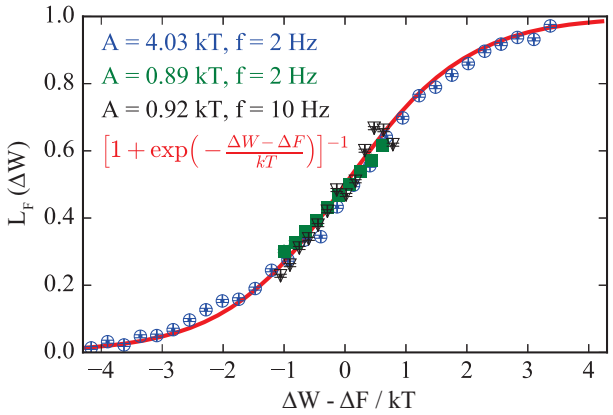

Figure 4 Arrow of time: the plot shows the likelihood $L(F)$ that a specific value ΔW is measured in a realization in the forward direction. The green, blue and black markers show values obtained from the experiment as described in Eq. (7) (with the error bars indicating the statistical error), while the red line shows the theoretical prediction according to Eq. (6). The green squares and black triangles correspond to the data shown in Fig. 3, panels (iii) and (iv), respectively.

The distribution shown in panel (iv) results from an even faster drive of $f = 10\,\mathrm{Hz}$. In this case, realizations with very few tunneling events are likely. For example, the peak at zero dissipation results from realizations like the one shown in Fig. 2b(iv), where no tunneling event occurs and $\mathrm{d}q/\mathrm{d}E = 0$ everywhere. On the other hand, realizations with finite but small dissipation become unlikely, because they require tunneling events to occur at $\mu \sim E_F$, where the drive is steepest. Hence, the peak in the distribution is a delta-peak. Steps are visible at $\Delta Q = \pm A$, as explained above, due to the sinusoidal waveform, which favors tunneling events at the beginning and end of the drive; and due to the unlikely initial condition required for $\Delta Q > A$. The distribution found here is very similar to that found in Ref. [18], though it is measured with a different drive amplitude.

5 Arrow of time The distributions in Fig. 3 show the presence of fluctuations in the heat dissipation in the dot–reservoir system which we study here. Using the thermodynamic state variable ΔU describing the change in internal energy, we can obtain the work $\Delta W = \Delta U - \Delta Q$ performed during any realization of the process, which allows us to study fluctuations in the work. These fluctuations can be used to quantify the notion of the arrow of time, as we describe in the following.

Imagine that we watch a movie of a system undergoing an irreversible, isothermal process, and we must guess whether the movie is being run in the "forward" or the "backward" direction. In this movie, we observe that an amount of work ΔW is performed on the system, and the free energy between the initial and final states of the system is ΔF. For a macroscopic system, if the inequality $\Delta W > \Delta F$ is satisfied then we can state with certainty that the movie is running forward in time, but if we observe $\Delta W < \Delta F$, then we conclude with equal confidence that the movie is being run backward in time. In other words, for large systems the arrow of time points in a direction specified by the second law of thermodynamics.

With small systems, where fluctuations dominate, this distinction becomes blurred. Nevertheless, we can quantify our ability to determine the direction of time's arrow [21]. Specifically, given values of ΔW and ΔF, the likelihood that the movie is being run forward is [33, 34]:

$$L(F) = \left[1 + e^{-\frac{(\Delta W - \Delta F)}{kT}}\right]^{-1}. \tag{6}$$

When $|\Delta W - \Delta F| \gg kT$, this result gives $L(F) \approx 1$ or $L(F) \approx 0$, in agreement with the macroscopic case. However, when ΔW is very close to ΔF, $L(F)$ takes on an intermediate value, reflecting the difficulty in distinguishing between forward and backward in time. We have used our data to test Eq. (6).

In our experiment, we drive the quantum dot in two directions, upwards ("forward") and downwards ("reverse") in energy, as shown in Fig. 2a. Each cycle of driving thus contains one realization of forward driving, followed by one realization of reverse driving. For each realization in the reverse direction, we multiply the work by -1, to obtain the value that we would observe if a movie of the process were run backward in time; in such a movie, it would appear that we are observing a realization of the forward process. By this procedure, from N cycles we obtain $2N$ values of ΔW, all of which putatively represent realizations of the forward process. Half of these work values are obtained from true realizations of the forward process; the other half are "fakes," coming from time-reversed realizations of the reverse process.

We binned both the forward ("true") and the backward ("fake") work values, letting $n_{\mathrm{fwd/bwd}}$ denote the number of forward/backward counts in a specified bin ΔW. For each bin, we then computed the fraction of forward counts:

$$p_{\mathrm{fwd}}(\Delta W) = \frac{n_{\mathrm{fwd}}(\Delta W)}{n_{\mathrm{fwd}}(\Delta W) + n_{\mathrm{bwd}}(\Delta W)}. \tag{7}$$

This fraction represents the empirical likelihood $L(F)$ that a work value ΔW is due to the forward (rather than a backward) realization of the process under study. The free energy difference has been computed analytically by utilizing the partition function of the system (Eq. (3)) and the relation $F = -kT\log(Z)$.

In Fig. 4, we plot the theoretical prediction, Eq. (6), as a solid red line together with the probability p_{fwd} obtained from experimental data with different drive parameters, but the same tunnel coupling $\Gamma = 42\,\mathrm{Hz}$. The data collapse onto a single curve given by Eq. (6), confirming that the form of this curve depends only on the temperature, and not on other parameters such as the amplitude and frequency of driving. The error bar denotes the error due to the finite statistics of few thousand realizations. An additional systematic

error occurs due to voltage drifts and the fluctuations in the electrostatic environment in the quantum dot. However, the good agreement between data and simulation shown in Fig. 3 suggest the systematic error to be small.

Mathematically, Eq. (6) is essentially a consequence of Crooks's fluctuation theorem [3, 4]. Conceptually, however, it is rather remarkable that the ability to distinguish the direction of time's arrow can be quantified by a formula as simple and universal as Eq. (6).

6 Conclusions We utilize a GaAs/AlGaAs quantum dot for measuring heat distributions in a small system, where fluctuations dominate and equilibrium predictions fail. By driving the quantum dot with different drive parameters, we show how the distributions of heat dissipation can deviate largely from the Gaussian form that arises near equilibrium. We characterize the work fluctuations in terms of the arrow of time and find that in small systems, the fluctuations blur the distinction between forward and backward realizations in a thermally broadened window of values for the work around the equilibrium free energy.

Acknowledgements We thank Jukka Pekola and Ivan Khaymovich for stimulating discussions. We greatfully acknowledge the U.S. National Science Foundation under grant DMR-1506969, the SNF and QSIT for providing the funding which enabled this work.

References

[1] L. Reichl, A Modern Course in Statistical Physics (Arnold, London, 1980).
[2] C. Jarzynski, Phys. Rev. Lett. **78**(14), 2690–2693 (1997).
[3] G. E. Crooks, Phys. Rev. E **60**(3), 2721–2726 (1999).
[4] G. E. Crooks, J. Stat. Phys. **90**(5–6), 1481–1487 (1998).
[5] M. Campisi, P. Talkner, and P. Hänggi, Phys. Rev. Lett. **102**(21), 210401 (2009).
[6] P. Talkner and P. Hänggi, J. Phys. A **40**(26), F569 (2007).
[7] T. Albash, D. A. Lidar, M. Marvian, and P. Zanardi, Phys. Rev. E **88**(3), 032146 (2013).
[8] A. E. Rastegin and K. Życzkowski, Phys. Rev. E **89**(1), 012127 (2014).
[9] D. Collin, F. Ritort, C. Jarzynski, S. B. Smith, I. Tinoco, and C. Bustamante, Nature **437**(7056), 231–234 (2005).
[10] O. P. Saira, Y. Yoon, T. Tanttu, M. Möttönen, D. V. Averin, and J. P. Pekola, Phys. Rev. Lett. **109**(18), 180601 (2012).
[11] J. Liphardt, S. Dumont, S. B. Smith, I. Tinoco, and C. Bustamante, Science **296**(5574), 1832–1835 (2002).
[12] B. Küng, C. Rössler, M. Beck, M. Marthaler, D. S. Golubev, Y. Utsumi, T. Ihn, and K. Ensslin, Phys. Rev. X **2**(1), 011001 (2012).
[13] D. M. Carberry, J. C. Reid, G. M. Wang, E. M. Sevick, D. J. Searles, and D. J. Evans, Phys. Rev. Lett. **92**(14), 140601 (2004).
[14] V. Blickle, T. Speck, L. Helden, U. Seifert, and C. Bechinger, Phys. Rev. Lett. **96**(7), 070603 (2006).
[15] G. M. Wang, E. M. Sevick, E. Mittag, D. J. Searles, and D. J. Evans, Phys. Rev. Lett. **89**(5), 050601 (2002).
[16] F. Douarche, S. Ciliberto, A. Petrosyan, and I. Rabbiosi, Europhys. Lett. **70**(5), 593 (2005).
[17] J. V. Koski, T. Sagawa, O. P. Saira, Y. Yoon, A. Kutvonen, P. Solinas, M. Möttönen, T. Ala-Nissila, and J. P. Pekola, Nature Phys. **9**(10), 644–648 (2013).
[18] A. Hofmann, V. F. Maisi, C. Rössler, J. Basset, T. Krähenmann, P. Märki, T. Ihn, K. Ensslin, C. Reichl, and W. Wegscheider, Phys. Rev. B **93**(3), 035425 (2016).
[19] S. An, J. N. Zhang, M. Um, D. Lv, Y. Lu, J. Zhang, Z. Q. Yin, H. T. Quan, and K. Kim, Nature Phys. **11**(2), 193–199 (2015).
[20] T. B. Batalho, A. M. Souza, L. Mazzola, R. Auccaise, R. S. Sarthour, I. S. Oliveira, J. Goold, G. De Chiara, M. Paternostro, and R. M. Serra, Phys. Rev. Lett. **113**(14) (2014).
[21] C. Jarzynski, Annu. Rev. Condens. Matter Phys. **2**(1), 329–351 (2011).
[22] R. Schleser, E. Ruh, T. Ihn, K. Ensslin, D. C. Driscoll, and A. C. Gossard, Appl. Phys. Lett. **85**(11), 2005–2007 (2004).
[23] L. M. K. Vandersypen, J. M. Elzerman, R. N. Schouten, L. H. W. v. Beveren, R. Hanson, and L. P. Kouwenhoven, Appl. Phys. Lett. **85**(19), 4394–4396 (2004).
[24] C. W. J. Beenakker, Phys. Rev. B **44**(4), 1646–1656 (1991).
[25] T. Ihn, Semiconductor Nanostructures: Quantum States and Electronic Transport (Oxford University Press, Oxford, 2010).
[26] M. Ciorga, A. S. Sachrajda, P. Hawrylak, C. Gould, P. Zawadzki, S. Jullian, Y. Feng, and Z. Wasilewski, Phys. Rev. B **61**(24), R16315–R16318 (2000).
[27] S. Tarucha, D. G. Austing, T. Honda, R. J. van der Hage, and L. P. Kouwenhoven, Phys. Rev. Lett. **77**(17), 3613–3616 (1996).
[28] T. Fujisawa, T. Hayashi, R. Tomita, and Y. Hirayama, Science **312**(5780), 1634–1636 (2006).
[29] K. MacLean, S. Amasha, I. P. Radu, D. M. Zumbühl, M. A. Kastner, M. P. Hanson, and A. C. Gossard, Phys. Rev. Lett. **98**(3), 036802 (2007).
[30] J. P. Pekola and O. P. Saira, J. Low-Temp. Phys. **169**(1-2), 70–76 (2012).
[31] D. V. Averin and J. P. Pekola, Europhys. Lett. **96**(6), 67004 (2011).
[32] H. Nyquist, Phys. Rev. **32**(1), 110–113 (1928).
[33] M. R. Shirts, E. Bair, G. Hooker, and V. S. Pande, Phys. Rev. Lett. **91**(14), 140601 (2003).
[34] P. Maragakis, F. Ritort, C. Bustamante, M. Karplus, and G. E. Crooks, J. Chem. Phys. **129**(2), 024102 (2008).